ELSEVIER

Polymer 43 (2002) 5535–5543

polymer

www.elsevier.com/locate/polymer

Formation of bubbles during ultrasonic treatment of cured poly(dimethyl siloxane)

Sang Eun Shim, Sayata Ghose, Avraam I. Isayev*

Institute of Polymer Engineering, The University of Akron, Akron, OH 44325-0301, USA

Received 7 March 2002; received in revised form 5 June 2002; accepted 10 June 2002

Abstract

A static ultrasonic treatment device was used to investigate the effect of ultrasound on degradation of unfilled poly(dimethyl siloxane) (PDMS) vulcanizate in the absence of shearing effect. The effects of pressure, ultrasound intensity and thickness of the disks upon ultrasonic treatment were investigated. The power consumption was measured as a function of sample thickness, ultrasonic amplitude, and applied pressure. The dynamics of bubble (nucleation, growth and coalescence) was also studied with respect to applied pressure and amplitude. An increase in thickness of the sample was observed during ultrasonic treatment. The unique correlation between gel fraction and crosslink density obtained in the present static experiments was compared with those of continuous devulcanization studied earlier. © 2002 Elsevier Science Ltd. All rights reserved.

Keywords: Poly(dimethyl siloxane); Bubbles; Ultrasound

1. Introduction

The first reported investigation of the degradation of polymers in solutions by ultrasound dates back to 1939 [1]. This topic has resurfaced over the past several decades and a number of studies have been carried out and reported [2–6]. Recently, Price presented an extensive compilation of the effects of ultrasound on polymers [7].

The use of high-intensity ultrasound in processing is generally based on the application of non-linear effects produced by finite amplitude pressure variations. The most important effects produced by ultrasound are: heat, cavitation, agitation, acoustic streaming, interface instabilities and friction, diffusion and mechanical rupture [8,9]. Due to its powerful mechanical and chemical effects, ultrasound has been used in diverse areas including sonochemical polymerization [10–13], sonochemical modification of polymer surfaces [14] cleavage of polymer chains in solution [15–17], dispersion of fillers and other components into polymers matrix such as in the formation of paints [18], the encapsulation of inorganic particles with polymers [19], and modification of particle size in polymer powders [20].

The application of powerful ultrasound for breaking down the rubber network is the most recent approach in the recycling of cured elastomeric materials. This process has various advantages in rubber recycling over other methods [21]. Since the invention of a continuous process of devulcanization of elastomers by means of an extruder with ultrasonic device attachment, devulcanization of various vulcanizates has been extensively studied including ground tire rubber (GRT) [21–27], styrene–butadiene rubber (SBR) [28–34], natural rubber (NR) [35–37], silicone rubber [38–40]. Use of devulcanized tire rubber in making rubber/plastic blends has been also investigated [41,42].

The effects of ultrasound on chemical transformations are not the result of any direct coupling of the sound field with the chemical species involved on a molecular level. The reason why ultrasound is able to produce chemical effects is due to the phenomenon of cavitation. Cavitation is the production of microbubbles and their motion in a medium when a large negative pressure is created [43]. Theoretical calculations indicate that for pure water the negative pressure required is about 1000 atm [43] for bubbles filled with vapor. Practically, cavitation can be produced at a considerably lower applied acoustic pressure due to the presence of weak spots in the liquid. Weak spots include the presence of gas nuclei in the form of dissolved gases, minute suspended gas bubbles, or tiny suspended particles. When produced in a sound field at sufficiently high power, the formation of cavitation bubbles will be initiated

* Corresponding author. Tel.: +1-330-972-6673; fax: +1-330-258-2339.
E-mail address: aisayev@uakron.edu (A.I. Isayev).

PII: S0032-3861(02)00392-0

during the rarefaction cycle. The acoustic field experienced by an individual bubble is not stable because of the interference of other bubbles forming and resonating around it. As a result some bubbles suffer sudden expansion to an unstable size and collapse violently. When they collapse, tremendous energy is released and various chemical and mechanical effects take place.

There are several theories which have been advanced to explain the energy release involved with cavitation of which the most understandable is the 'hot spot' approach [44]. Each cavitation bubble acts as a localized microreactor which, in aqueous systems, generates instantaneous temperatures of roughly 5000 °C, pressure in excess of about 1000 atm, and heating and cooling rates above 10^{10} K/s [44,45].

The major difference between breakage of polymers in solution under ultrasound and the thermal degradation process is the *loci* of chain scission. Ultrasonic chain scission is characterized as 'non-random' which means that the cleavage of polymeric chains preferentially takes place near the middle of the chain compared to random scission upon thermal degradation [46].

The clear mechanism of ultrasonic degradation of crosslinked elastomers is still in question. However, it is believed that most of the physical effects caused by ultrasound are usually attributed to cavitation, the rapid growth and contraction of microbubbles as the high intensity sound wave propagates in the rubber [23,47,48] This effect is in contrast to the cavitational collapse in polymer solutions [7].

The proposed devulcanization model [23] is based upon a mechanism of rubber network breakdown caused by ultrasonic cavitation, which is created by high intensity ultrasonic waves in the presence of pressure and heat. It is well known that some amount of cavities or small bubbles are present in rubber during any type of rubber processing [47]. Driven by ultrasound, the cavities pulsate with amplitude depending mostly upon the difference between ambient and ultrasonic pressures (acoustic cavitation). The devulcanization of rubber network can occur primarily around pulsating cavities due to the highest level of strain produced by the powerful ultrasound [48].

In this study, a static ultrasonic treatment device was used to investigate the effect of ultrasound on degradation of unfilled poly(dimethyl siloxane) (PDMS) vulcanizate in the absence of shearing effect. The effects of pressure, ultrasound intensity and thickness of the disks upon ultrasonic treatment were investigated. The dynamics of bubble nucleation, growth and coalescence were studied. The unique correlation between gel fraction and crosslink density obtained in the present static experiments was compared to those of continuous devulcanization studied earlier [40].

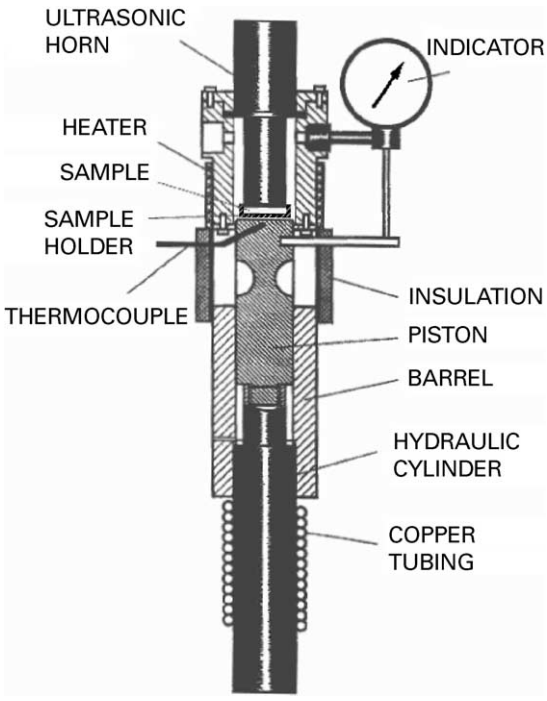

Fig. 1. Schematic drawing of the static ultrasound device.

2. Experiment

2.1. Sample preparation

A polymeric network was prepared by crosslinking PDMS, SE 64 made by General Electric Company with weight-average molecular weight $M_w = 4.14 \times 10^5$ and number-average molecular weight $M_n = 2.34 \times 10^5$ (measured by gel permeation chromatography, GPC). It contained 0.6 mol% vinyl groups. Dicumyl peroxide (DCP), LUPEROX® 500R (Pennwalt Corp.), was used as the curative. 0.5 phr DCP was mixed with PDMS on the two-roll mill at 25 °C. After mixing, the rubber slabs having 0.63 and 1.80 mm thickness were pre-cured by a compression molding press (Wabash) at 170 °C for 10 min and then post-cured in a ventilated oven at 200 °C for 2 h in order to remove volatile by-products generated by decomposition of the peroxide. The rubber disks with a diameter of 25.4 mm were made by punching out the cured slabs with an arch punch. The accuracy in thickness of each specimen was within ±3%

2.2. Ultrasonic devulcanization

Fig. 1 shows a schematic of the static ultrasonic device. The ultrasonic unit is fixed on the main frame of the machine while a piston moves up and down by a hydraulic fluid. The rubber specimen is placed between the ultrasonic horn and the piston and a certain pressure is the applied to rubber by the movable piston.

A 3000 W ultrasonic power supply, a converter and a booster were used to provide longitudinal vibrations to the

Table 1
Comparison of experimental parameters in dynamic and static devulcanization

Parameters	Dynamic [40,49]	Static
Thickness of sample (mm)	0.35, 0.63	0.63, 1.80
Pressure (MPa)	1.0–5.8	0.34–1.03
Ultrasound intensity (μm)	5–10	10–30
Residence or exposure time (s)	1.4–10.0[a]	5.0–40.0

[a] Average values.

horn at a frequency of 20 kHz. The amplitudes, A, of the ultrasonic wave were 10, 20, 25, and 30 μm. The ultrasound exposure time was varied from 5 to 40 s. It is noted that more prolonged application of ultrasound on sample caused a disintegration of the sample so it was hard to collect specimen from the sample holder cup. The value of ultrasonic power consumption in watt was read from power meter connected to an ultrasound generator.

The applied pressure was 0.34, 0.69, and 1.03 MPa. The setting pressure was kept constant throughout the experiment. All the experiments were done at room temperature to see the temperature change from ambient temperature. Temperature build-up due to heat dissipation from ultrasound was recorded by inserting a thermocouple on the wall of the sample holder. In addition, the amount of squeezed material, thickness change of the sample and energy consumed were measured for each condition. The ultrasonically treated silicone rubber samples were collected for further investigation.

The experimental parameters in this static mode are compared with those in the dynamic devulcanization in extruder [40,49] in Table 1. The sample thickness of 0.63 mm was the same as the distance between the die and the flat surface of ultrasound horn in dynamic devulcanization of PDMS in extruder. In static experiments, the imposed pressures (0.34–1.03 MPa) were within those imposed in extrusion experiments (1.0–5.8 MPa). The maximum pressure imposed in the static device was limited to 1.03 MPa. Imposition of higher pressure led to breakage of the sample. However, higher ultrasound amplitude was applied in static experiments in order to obtain the formation of bubbles at these low applied pressures.

2.3. Bubble evolution, and thickness change

After samples were exposed to ultrasound for certain period of time under pressure, digital images of each specimen were taken on the samples removed from the sample holder. The number and average sizes of created bubbles were analyzed by Scion Image Analyzer® on IBM compatible platform computer. The number of visible bubbles was counted from the digital image and the two dimensional areas of the bubbles were obtained and their diameters were calculated from the program.

The change of the sample thickness during the application of ultrasound was measured by a thickness gauge indicator (with precision of 0.0254 mm) attached on top of the sample holder as shown in Fig. 1. When the probe of the thickness gauge contacted the top surface of a sample in the sample holder, the indicator was set to zero. Therefore, the change in thickness during experiment was instantly measured from the indicator.

2.4. Structural characterization

Gel fractions of the vulcanized and devulcanized samples were measured by Soxhlet extraction, using benzene as the solvent. The extraction time was set at 24 h. Crosslink densities of the gel were determined by the swelling method. The weights of the swollen samples were measured after removing the surface solvent. Then the samples were dried in a vacuum oven at 50 °C for 24 h and were weighed again. The crosslink density, n_c, was calculated using Flory–Rehner equation [50].

$$n_c = -\frac{\ln(1 - V_r) + V_r + \chi V_r^2}{V_1(V_r^{1/3} - V_r/2)} \quad (1)$$

where n_c is the effective number of chains in a real network per unit volume, V_1 the molecular volume of the solvent ($V_1 = 89.1$ cm^3/mol), χ the solubility parameter between a network and solvent, V_r is the volume fraction of the polymer in the swollen network in equilibrium with the pure solvent. The volume fraction of the rubber network in the swollen phase is calculated from the equilibrium swelling data. For the PDMS and benzene system used in this study, χ is 0.5 [51].

3. Results and discussion

3.1. Power consumption

Fig. 2 shows the effect of ultrasonic amplitude and applied pressure on power consumption. Since different samples were used for each interval of ultrasound exposure, the power consumption values recorded were the average of those measured at 5, 10, 20 and 40 s. It should be noted that the power consumption at different exposure times varied by about 10%. In our previous study on SBR carried out using a static ultrasonic treatment [52], the applied pressure continuously decayed during ultrasound treatment, which led to a decrease in power consumption with ultrasound exposure time. So the substantial influence of ultrasound in the previous experiments on SBR with decay of pressure and power consumption was difficult to interpret. However, the applied pressure was held constant in this study and therefore the level of energy consumption remained unchanged during ultrasonic treatment.

In Fig. 2(a), power consumption increases with applied ultrasonic amplitude, since more ultrasonic energy is

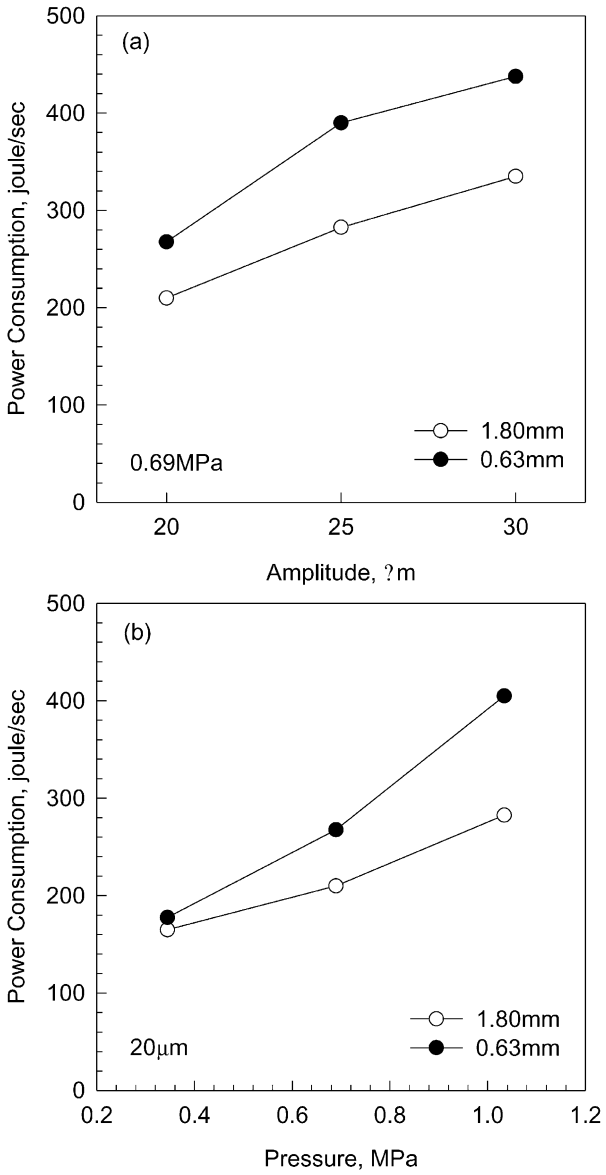

Fig. 2. The effects of ultrasonic amplitude at a constant pressure of 0.69 MPa (a), and pressure at a constant amplitude of 20 μm (b) on power consumption in static condition.

consumed at higher amplitude in the process of devulcanization. The power consumption also increases with applied pressure (Fig. 2(b)). The difference of energy used becomes greater with increasing pressure for 0.63 and 1.80 mm disks indicating that the applied pressure is evidently one of the major factors influencing the degree of devulcanization as well as amplitude at a specific time. For all cases, energy consumption for disks of 0.63 mm thickness was always higher than that of 1.80 mm thickness since strain amplitude and ultrasonic energy intensity per volume is higher in thin specimens.

3.2. Temperature, squeezed sol, and thickness

Fig. 3 shows the temperature build-up caused by the

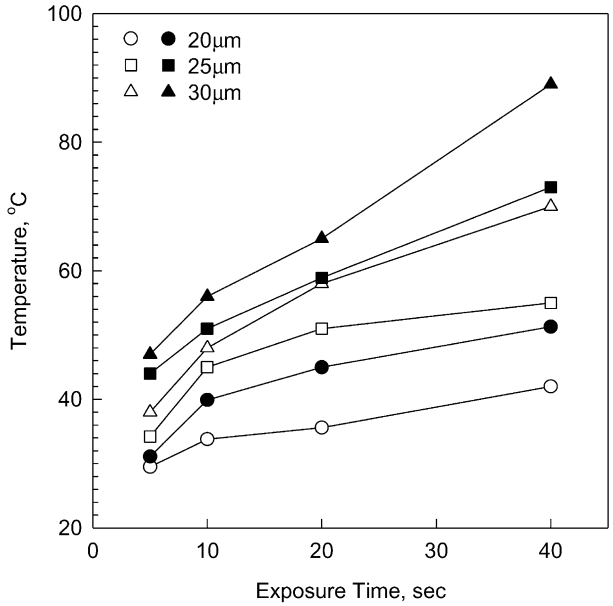

Fig. 3. Temperature buildup as a function of ultrasonic exposure time at various amplitudes and pressure of 0.69 MPa, (open symbols: 1.80 mm, solid symbols: 0.63 mm).

dissipation of ultrasonic energy through polymeric media. The temperature increase in the ultrasonic degradation of polymer in solutions has not been observed [7]. However, in the case of ultrasonic degradation of polymer network in solid state, it is seen that significant amount of mechanical energy is converted into thermal energy as shown in Fig. 3. The simulation of temperature at tiny spots in liquid during ultrasonic sonication [44,45] indicates that ultrasonic cavitation does not occur under isothermal condition. In the early stage of ultrasonic exposure, the temperature rise is fast and then becomes slow with time. Temperature increases continuously with exposure time. The rise in temperature for thin disks is higher than that of thick ones. In addition, higher ultrasonic amplitude gives greater heat dissipation. This is directly related to the energy consumption in Fig. 2 by taking into account the fact that some part of ultrasonic energy is used for cavitation and the other is dissipated as heat. Therefore, higher level of energy input leads to higher dissipation of energy causing temperature buildup. Evidently, this is the main reason why in our earlier experiments the effect of the barrel temperature on the gel fraction and crosslink density of ultrasonically treated unfilled silicone rubber was found to be insignificant [52].

Upon ultrasonic treatment sol is created due to the breakup of main chains and crosslinks. A fraction of the sol is squeezed from the sample due to the imposed pressure. The remainder of the sol is trapped in the sample. Fig. 4 shows the amount of squeezed sol in percentage based on the total amount of each specimen after ultrasonic exposure as a function of ultrasonic exposure time for rubber disks having two different thicknesses. As expected, the amount of squeezed sol increases with increase in the exposure time and ultrasonic amplitudes. In addition, the amount of

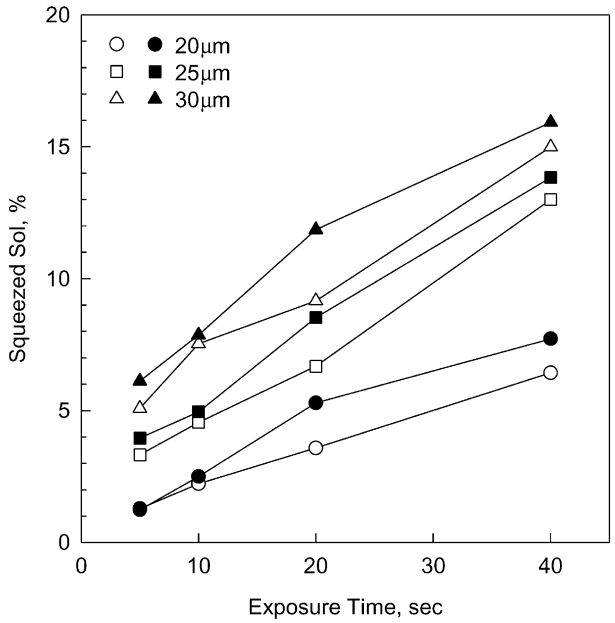

Fig. 4. The amount of squeezed sol as a function of ultrasonic exposure time at various ultrasonic amplitudes at 0.69 MPa, (open symbols: 1.80 mm, solid symbols: 0.63 mm).

squeezed sol for 0.63 mm thick disks is always higher than 1.83 mm thick ones at the same conditions.

During ultrasonic treatment a phenomenon of an increase in thickness was observed when a constant static pressure was imposed. Fig. 5 shows the thickness increase while ultrasound is applied. It was seen that the thickness of the sample immediately increased to a certain level while ultrasound was on and went back to its original thickness after ultrasound was turned off. The thickness increase is higher at higher amplitude and tends to level off with prolonged time. This increase in thickness may be expostulated by the cavitation of bubbles in the sample and insufficient rigidity of the apparatus. As the amount of degraded low molecular weight species increases, the cavitation of voids or bubbles becomes facilitated due to the reduced viscosity of the medium which in turn leads to increase in thickness.

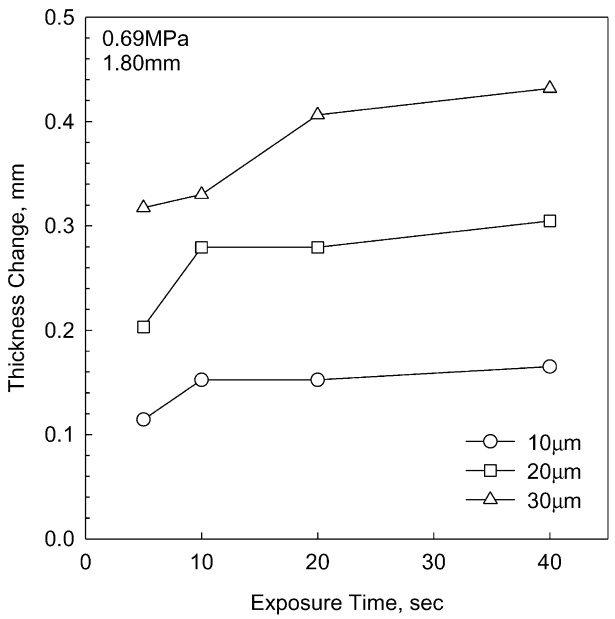

Fig. 5. The increase of thickness during the exposure of ultrasound of various amplitudes at pressure of 0.69 MPa.

3.3. Bubble formation

Fig. 6(a)–(e) are images of formed bubbles with varying time in 1.8 mm thick PDMS disks at a pressure of 0.69 MPa and at an ultrasonic amplitude of 20 μm. These pictures show very well the formation of bubbles, their growth and coalescence due to ultrasonic cavitation in crosslinked polymer. More details of bubble dynamics are shown in the following figures. In particular, Fig. 7 shows the change of number of bubbles with respect to ultrasound exposure time at various ultrasonic amplitudes at 0.69 MPa (a) and at various pressures and at a constant amplitude of 20 μm (b). In Fig. 7(a), interestingly the number of bubbles at low amplitude continues to increase at a short period of time up

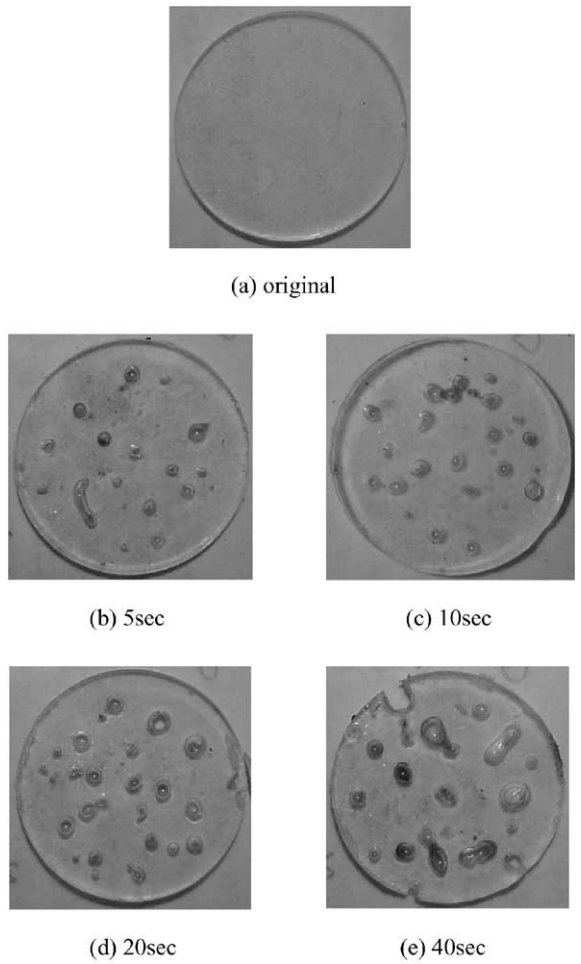

Fig. 6. Formation of bubbles in 1.8 mm thick PDMS disk at pressure of 0.69 MPa and at amplitude of 20 μm.

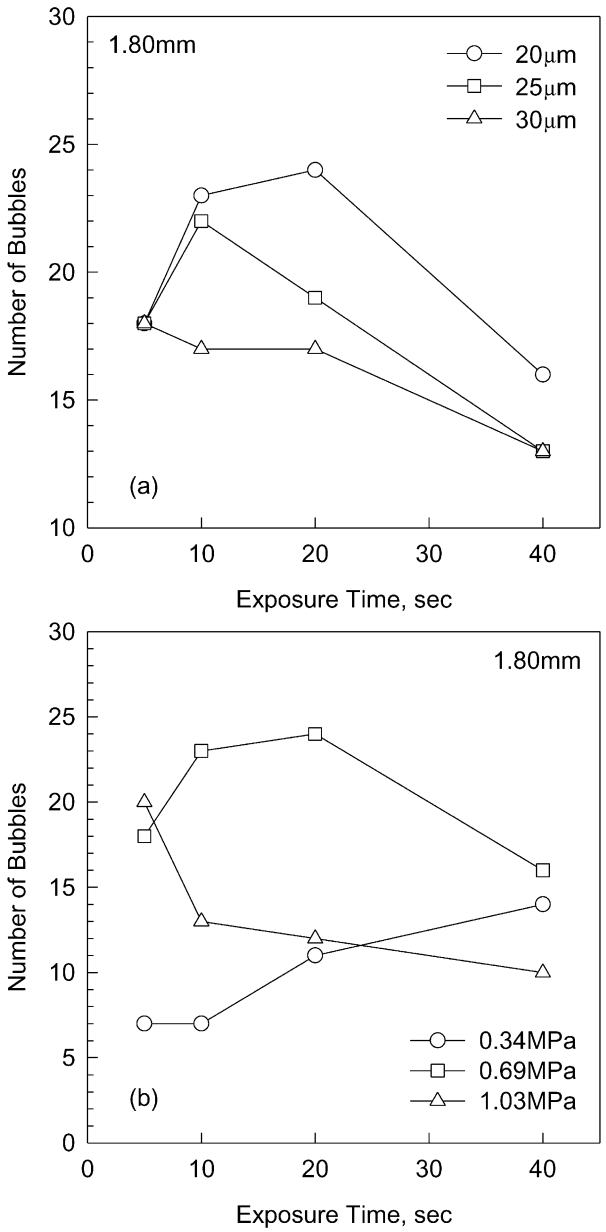

Fig. 7. Number of bubbles as a function of ultrasound exposure time at various amplitudes and pressure of 0.69 MPa (a) and various pressures and amplitude of 20 μm (b).

to 20 s and then finally decreases due to the coalescence of bubbles. Again bubbles at 30 μm start to coalesce at an early stage. This implies that ultrasonic intensity has significant effect on bubble dynamics. Fig. 7(b) shows that pressure is one of the important factors in bubble formation due to ultrasound. Here the number of bubbles is very distinct according to the level of applied pressure. At the lowest pressure (0.34 MPa), the number of bubbles tends to increase with exposure time without significant coalescence. At the highest pressure (1.03 MPa), the number of bubbles immediately decreases when ultrasound is imposed. At an intermediate pressure (0.69 MPa), the number of bubbles increases at an early stage due to the accelerated nucleation and the bubbles go through coalescence at prolonged time. In addition, one can see from Fig. 7(b) that the initial number of bubbles at different levels of pressure is higher at higher pressures due to the ease of nucleation at higher pressure at the early stage of ultrasonic treatment.

In Fig. 8 the average diameters of bubbles are measured as a function of exposure time. Fig. 8(a) shows the effect of ultrasonic amplitude at a constant pressure of 0.69 MPa. Fig. 8(b) shows the effect of applied pressure at a constant amplitude of 20 μm on the average size of bubbles. In Fig. 8(a), size of bubbles is increased with time at all conditions due to coalescence except at the initial stage of 25 μm where the nucleation of bubbles is favored rather

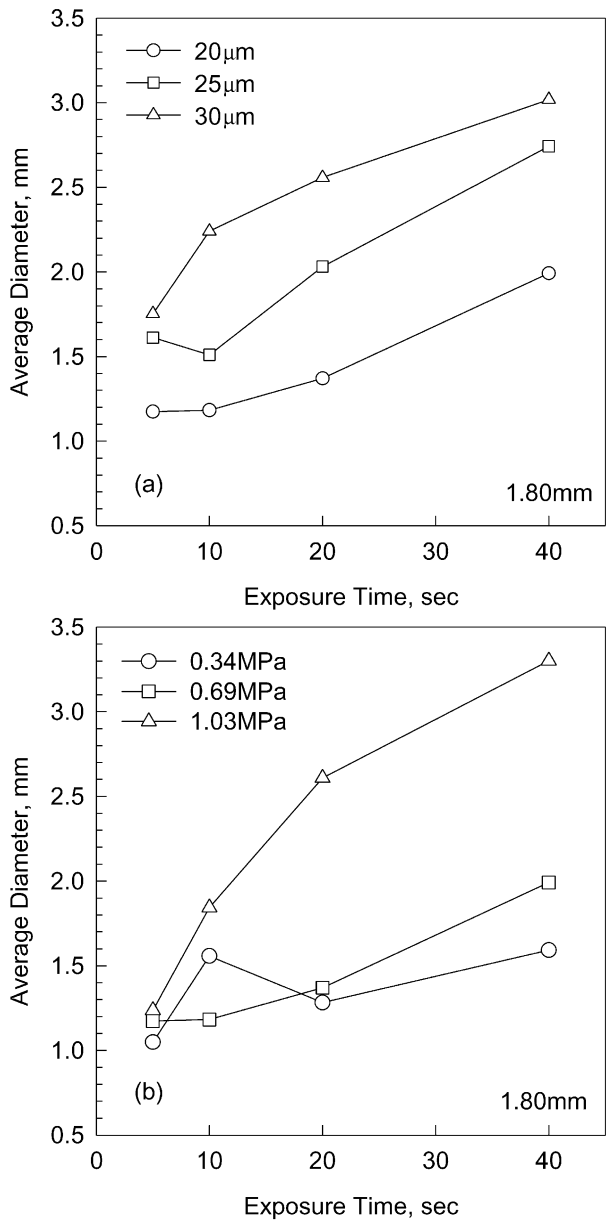

Fig. 8. Average size of bubbles as a function of ultrasound exposure time at various amplitudes and pressure of 0.69 MPa (a) and various pressures and amplitude of 20 μm (b).

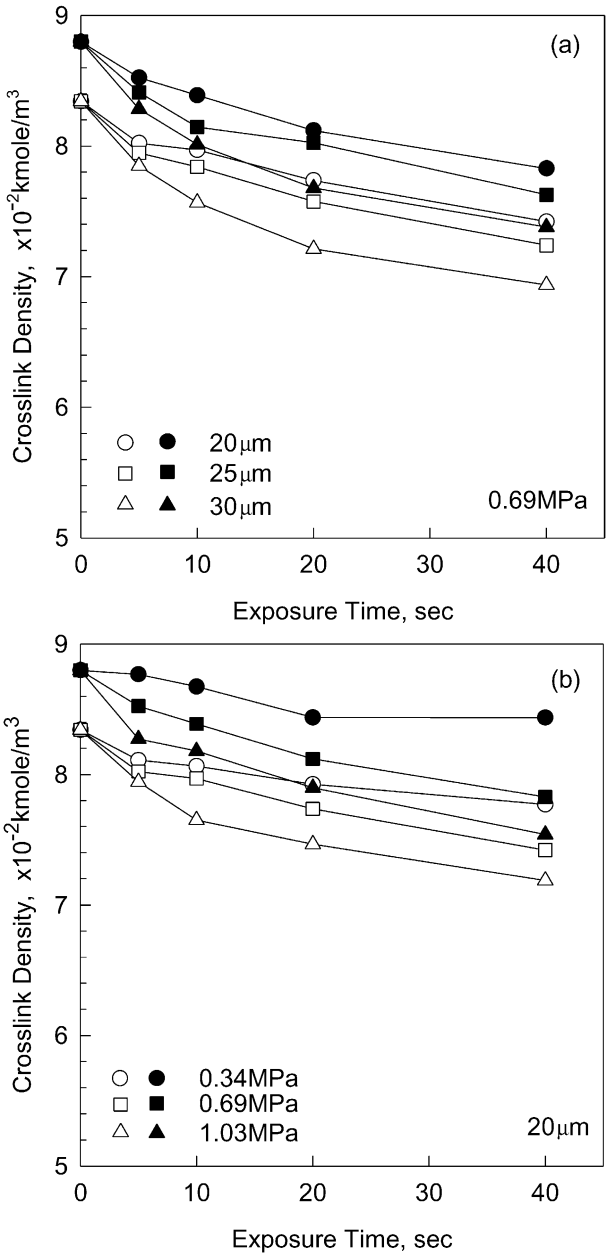

Fig. 9. Crosslink density as a function of exposure time at various amplitudes and pressure of 0.69 MPa (a), at various pressures and amplitude of 20 μm (b) (open symbols: 1.80 mm, solid symbols: 0.63 mm).

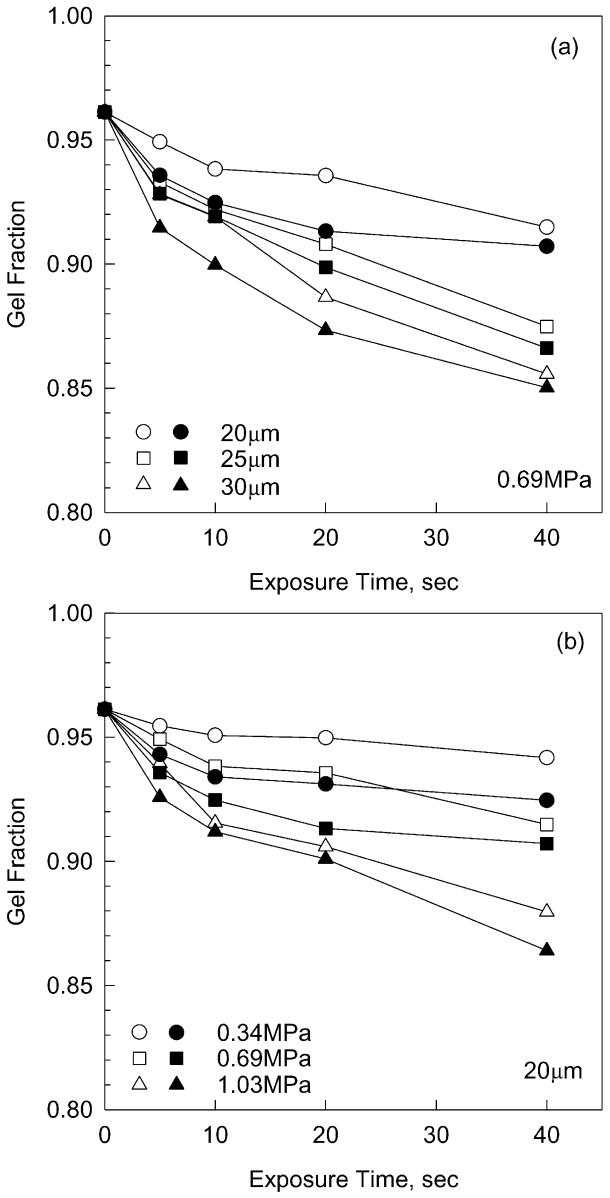

Fig. 10. Gel fraction as a function of exposure time at various amplitudes and pressure of 0.69 MPa (a), and at various pressures and amplitude of 20 μm (b) (open symbols: 1.80 mm, solid symbols: 0.63 mm).

than coalescence. The sample treated for 5 s shows that a higher amplitude generates larger bubbles possibly by coalescence of invisibly tiny bubbles. As shown in Fig. 8(b), the average size of bubbles at a higher pressure is higher than that at low pressure. This can be explained by the fact that at higher pressure bubbles grow more easily by coalescence.

3.4. Crosslink density and gel fraction

Figs. 9 and 10 show the change of crosslink density and gel fraction as a function of ultrasonic exposure time at various ultrasonic amplitudes and applied pressures, respectively. It is noted that the initial crosslink density for the 0.63 mm thick samples is higher than that of the 1.80 mm ones while gel fractions are the same for both. The lower crosslink in a 1.80 mm thick disk arises from the heat transfer which might cause non-uniformity along the height direction of the samples because the same curing time was applied for 0.63 and 1.80 mm samples. The effects of amplitude are similar on both thin and thick disks and higher ultrasound leads to lower crosslink density and gel fraction. Pressure has similar effects as ultrasonic amplitude. Higher applied pressure causes a greater decrease of crosslink density and gel fraction. For 1.8 mm thick specimens, when applied pressure is 0.34 MPa, a little decrease in crosslink density and gel fraction is observed.

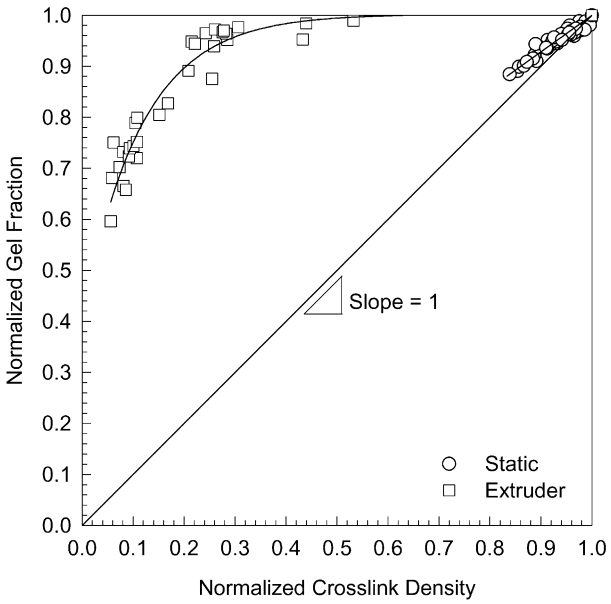

Fig. 11. Normalized gel fraction vs. normalized crosslink density obtained in continuous devulcanization process and static conditions.

Fig. 11 shows a normalized gel fraction vs. normalized crosslink density plot. Normalized values are ratios of current values of treated sample to those of initial values the sample. Here data points denoted by rectangular symbols were obtained from devulcanization experiments on unfilled cured silicone rubber by means of the single screw rubber extruder with ultrasonic die attachment. In these experiments ultrasonic treatment takes place in the presence of shear stresses due to the flow of material [40]. The average residence times in these earlier experiments were in the range 1.4–10 s (Table 1) which are within the ultrasonic exposure times of the present static experiments. Results obtained from static experiments are shown by circular symbols. Unique curves are obtained for both dynamic and static experiments [48]. The decrease in normalized crosslink density and normalized gel fraction is much higher in dynamic case than in static condition. This implies that ultrasonic treatment in dynamic condition breaks mostly crosslinks. The slope of line of dependence of normalized gel fraction vs. crosslink density obtained from static treatment is close to unity. Therefore one can conclude that the same amount of chemical bonds in PDMS backbone is severed in static conditions as those in crosslinks. This causes random degradation of PDMS chains in static treatment rather than selective devulcanization.

4. Conclusions

The degradation of unfilled PDMS vulcanizate in bulk state by ultrasound has been investigated in the absence of shear. The power consumption results show that higher energy is required to break chains in thinner samples. Pressure is found to be an important factor in the process. As the applied pressure increases, more energy is consumed. At low pressure, the difference in power consumption for thin and thick samples is small and becomes higher as higher pressure is applied. Since some amount of energy dissipates into heat, the overall temperature of the sample continues to increase as ultrasonic exposure time is prolonged. At the same amplitude, temperature increase in thin sample is higher than that in thick samples because more energy is used in thinner samples. The amount of squeezed sol due to degradation of PDMS molecules is also increased with the power consumption and temperature buildup. Therefore higher the ultrasonic amplitude and longer the ultrasonic exposure time, more is the amount of squeezed sol. In addition, this amount is higher for thin specimens than for thick ones.

The observation of bubble formation reveals that the number of bubbles initially increases due to nucleation and decreases through coalescence among bubbles. At low amplitude and low pressure, it is shown that the nucleation process is more likely favored resulting in an increase in the number of bubbles. However, the coalescence process is favored at higher amplitude and pressure leading to a decrease in the number of bubbles. Once bubbles are created, they start to grow and new bubbles are generated at the same time. The average size of bubbles tends to increase based on this fact, but it decreases at certain conditions where nucleation is more likely favored.

The crosslink density and gel fraction show the effects of ultrasonic amplitude and applied pressure on chain scission. The normalized gel fraction vs. normalized crosslink density plot represents the fact that ultrasound mostly breaks crosslinks in the case of continuous ultrasonic devulcanization under dynamic condition where shearing and pressure forces are inevitably involved, while significant amount of main chains are subjected to rupture in the absence of shearing force in the case of static conditions.

Acknowledgments

This work is supported by grant DMI-0084740 from the National Science Foundation, Division of Engineering.

References

[1] Schmid G, Rommel O. Rupture of macromolecules with ultrasound. Z Phys Chem 1939;A185:97–139.
[2] El'psner IE. Ultrasound: physical, chemical and biological effects. New York: Consultant Bureau; 1964.
[3] Basedow AM, Ebert KH. Ultrasonic degradation of polymers in solution. Adv Polym Sci 1977;22:83–148.
[4] Suslik KS, editor. Ultrasound: its chemical, physical and biological effects. New York: VCH Publishers; 1988.
[5] Mason TJ, Lorimer JP. Sonochemistry: theory, applications and uses of ultrasound in chemistry. New York: Wiley; 1988.

[6] Mason TJ, editor. Advances in sonochemistry. London: JAI Press; 1990. p. 231.
[7] Price GJ. In: Crum LA, editor. Sonochemistry and sonoluminescences. Boston: Kluwer Academic Publishers; 1999. p. 321–44.
[8] Ensminger D. Ultrasonics. New York: Marcel Dekker; 1988.
[9] Gallego-Juarz JA. New technologies in high-power ultrasonic industrial applications. IEEE Ultrason Symp 1994;3:1334–52.
[10] Orszulik ST. The use of ultrasound and a thermolabile radical initiator in the polymerization of acrylate monomers. Polymer 1993;34: 1320–1.
[11] Price GJ, Norris DJ, West PJ. Polymerization of methyl methacrylate initiated by ultrasound. Macromolecules 1992;25:6447–54.
[12] Schultz DN, Sissano JA, Costello CA. Ultrasound assisted preparation and polymerization of anionic initiators. Polym Prepr 1994;35:514–5.
[13] Hatate Y, Ikari A, Kondo K, Nakashio F. Change of size distribution of polymer droplets with time in styrene suspension polymerization under ultrasonic irradiation. Chem Engng Commun 1985;34:325–33.
[14] Price GJ, Keen F, Clifton AA. Sonochemically-assisted modification of polyethylene surfaces. Macromolecules 1996;29:5664–70.
[15] Basedow AM, Ebert K. Ultrasonic degradation of polymers in solution. Adv Polym Sci 1977;22:83–148.
[16] Price GJ. The use of ultrasound for the controlled degradation of polymer solutions. Adv Sonochem 1990;1:231–87.
[17] Price GJ, Smith PF. Ultrasonic degradation of polymer solutions. III. The effect of changing solvent and solution concentration. Eur Polym J 1993;29:419–24.
[18] Stoffer JO, Fahim M. Ultrasonic dispersion of pigment in water based paints. J Coat Technol 1991;63:61–8.
[19] Lorimer JP, Mason JJ, Kershaw D, Livsey I, Templeton-Knight R. Effect of ultrasound on the encapsulation of titanium dioxide pigment. Colloid Polym Sci 1991;29:392–7.
[20] Price GJ, Clifton AA. Sonochemical acceleration of persulfate decomposition. Polymer 1996;37:3971–3.
[21] Isayev AI, Chen J, Tukachinsky A. Novel ultrasonic technology for devulcanization of waste rubbers. Rubber Chem Technol 1995;68: 267–80.
[22] Tukachinsky A, Schworm D, Isayev AI. Devulcanization of waste tire rubber by powerful ultrasound. Rubber Chem Technol 1996;69: 92–103.
[23] Isayev AI, Yushanov SP, Chen J. Ultrasonic devulcanization of rubber vulcanizates. Part 1: process model. J Appl Polym Sci 1996;59: 803–13.
[24] Isayev AI, Yushanov SP, Chen J. Ultrasonic devulcanization of rubber vulcanizates. Part 2: simulation and experiment. J Appl Polym Sci 1996;59:815–24.
[25] Isayev AI, Yushanov SP, Schworm D, Tukachinsky A. Modeling of ultrasonic devulcanization of tyre rubbers and comparison with experiments. Plast, Rubber Compos Process Appl 1996;24:1–12.
[26] Yushanov SP, Isayev AI, Levin VYu. Percolation simulation of the network degradation during ultrasonic devulcanization. J Polym Sci Phys Ed 1996;34:2409–18.
[27] Yun J, Oh JS, Isayev AI. Ultrasonic devulcanization reactors for recycling of GRT: comparative study. Rubber Chem Technol 2001; 74:317–30.
[28] Isayev AI, Yushanov SP, Kim SH, Levin VY. Ultrasonic devulcanization of waste rubbers: experimentation and modeling. Rheol Acta 1996;35:616–30.
[29] Levin VY, Kim SH, Massey J, von Meerwall E, Isayev AI. Ultrasound devulcanization of sulfur vulcanized SBR: crosslink density and molecular mobility. Rubber Chem Technol 1996;69:104–14.
[30] Johnston ST, Massey J, von Meerwall E, Kim SH, Levin VY, Isayev AI. Ultrasound devulcanization of SBR: molecular mobility of gel and sol. Rubber Chem Technol 1997;70:183–93.
[31] Isayev AI, Kim SH, Levin VY. Reclaimed SBR with superior mechanical properties. Rubber Chem Technol 1997;70:194–201.
[32] Levin VYu, Kim SH, Isayev AI. Effect of crosslink type on the ultrasound devulcanization of SBR vulcanizates. Rubber Chem Technol 1997;70:641–9.
[33] Levin VY, Kim SH, Isayev AI. Vulcanization of ultrasonically devulcanized SBR elastomers. Rubber Chem Technol 1997;70: 120–8. Gummi Fasern Kunststoffe 1998;51:898–905.
[34] Yushanov SP, Isayev AI, Kim SH. Ultrasonic devulcanization of SBR rubber: experimentation and modeling based on cavitation and percolation theories. Rubber Chem Technol 1998;71:168–90.
[35] Tapale M, Isayev AI. Continuous ultrasonic devulcanization of unfilled NR vulcanizates. J Appl Polym Sci 1998;70:2007–19.
[36] Hong CK, Isayev AI. Continuous ultrasonic devulcanization of carbon black filled NR vulcanizates. J Appl Polym Sci 2001;79:2340–8.
[37] Hong CK, Isayev AI. Blends of ultrasonically devulcanized and virgin carbon black filled NR. J Mater Sci 2002;37:1–4.
[38] Diao B, Isayev AI, Levin VYu, Kim SH. Surface behavior of blends of SBR with ultrasonically devulacanized silicone rubber. J Appl Polym Sci 1998;69:2691–6.
[39] Diao B, Isayev AI, Levin VY. Basic study of continuous ultrasonic devulcanization of silicone rubber. Rubber Chem Technol 1999;72: 152–64. Gummi Kunstst 1999;52:438–45.
[40] Shim SE, Isayev AI. Ultrasonic devulcanization of precipitated silica filled silicone rubber. Rubber Chem Technol 2001;74:303–16.
[41] Luo T, Isayev AI. Rubber/plastic blends based on devulcanized ground tire rubber. J Elast Plast 1998;30:133–60.
[42] Hong CK, Isayev AI. Plastic/rubber blends of ultrasonically devulcanized GRT with HDPE. J Elastom Plast 2001;33:47–71.
[43] Mason TJ. Sonochemistry. New York: Oxford University Press; 1999. Chapter 1.
[44] Suslick KS, Cline RE, Hammerton DA. Sonochemical hot spot. J Am Chem Soc 1986;108:5641–2.
[45] Henglein A. Sonochemistry: historical developments and modern aspects. Ultrasonics 1987;25:6–16.
[46] Glynn PAR, Van der Hoff BME. Degradation of polystyrene in solution by ultrasonation. Molecular weight distribution study. J Macromol Sci Chem 1973;7:1695–719.
[47] Yashin VV, Isayev AI. A model for rubber degradation under ultrasonic treatment. Part I: acoustic cavitation in viscoelastic solid. Rubber Chem Technol 1999;72:741–57.
[48] Yashin VV, Isayev AI. A model of rubber degradation under ultrasonic treatment. Part II: rupture of rubber network and comparison with experiments. Rubber Chem Technol 2000;73: 325–39.
[49] Diao B. Basic study of continuous ultrasonic devulcanization of unfilled silicone rubber. MS Thesis, The University of Akron; 1997. p. 59.
[50] Flory PJ, Rehner Jr. J. Statistical mechanics of cross-linked polymer networks. II. Swelling. J Chem Phys 1943;11:521–6.
[51] Brandrup J, Immergut EH, Grulke EA, editors. Polymer handbook, 4th ed. New York: Wiley; 1999. p. 252.
[52] Hong CK, Isayev AI. Ultrasonic devulcanization of unfilled SBR under static and continuous conditions. Rubber Chem Technol 2002; 75:1.